Kinetics of Precipitation of Surfactants. II. Anionic Surfactant Mixtures

Cheryl H. Rodriguez and John F. Scamehorn*

Institute for Applied Surfactant Research, The University of Oklahoma, Norman, Oklahoma 73019

ABSTRACT: Precipitation kinetics were measured for calcium-induced precipitation of mixtures of two anionic surfactants. The overall time required for precipitation to occur increased dramatically in specific ranges of compositions for the surfactant mixtures when compared to single components. Adsorption of the nonprecipitating surfactant onto the precipitate surface was shown to be responsible for this remarkable synergism. The higher the supersaturation of surfactant monomers, the more rapidly precipitation occurred. Under conditions where both surfactants were supersaturated, precipitation sometimes occurred in stepwise fashion, where crystals of different composition were formed with different induction times. Image analysis of the crystalline precipitate showed that crystal habit was affected when the two surfactants were mixed, indicating that processes such as adsorption and coprecipitation (most likely by inclusion) were occurring. When the crystals were allowed to age in solution for a period of 1 wk, the crystalline phase from the mixed surfactant solutions was found to separate into two types of crystals, which resembled week-old crystals formed from single surfactant systems.

Paper no. S1167 in *JSD 4*, 15–26 (January 2001).

KEY WORDS: Anionic surfactants, calorimetry, kinetics of precipitation, supersaturation, surfactant mixtures, surfactant precipitation.

An important characteristic of anionic surfactants that can inhibit their use in many applications is their tendency to precipitate from aqueous solutions. One condition that can cause anionic surfactants to precipitate readily is hard water (water containing multivalent cations). Precipitation of surfactants due to hard water can be detrimental in applications such as detergency, where precipitated surfactant is not available for participation in the cleaning process. There have been numerous studies of the thermodynamics of surfactant precipitation. However, there have been very few investigations of the kinetics or rate of surfactant precipitation despite the fact that many practical surfactant processes may be far from equilibrium. Since the vast majority of surfactants in industrial or consumer products are mixtures of surfactant molecular structures, the effect of mixture composition on precipitation kinetics has important consequences for applications.

One purpose of this study is to address a paradox of fundamental significance and practical importance. Single, isomerically pure anionic surfactants are generally precipitated to equilibrium with calcium in a few minutes (1–3). Yet commercial detergents are known anecdotally to remain supersaturated for long periods of time (even weeks or months). It has been suspected that this apparent inconsistency is due to the use of complex surfactant mixtures in commercial products. Hence this study is a systematic investigation of the effect of mixing two pure anionic surfactants on the kinetics of precipitation by calcium.

The kinetics of precipitation of single anionic surfactants with calcium and of anionic surfactants with cationic surfactants has been investigated (1). In this study, the kinetics of anionic surfactant precipitation from anionic surfactant mixtures by calcium is studied both above and below the critical micelle concentration (CMC). Precipitate crystal habit for single and mixed surfactant systems is qualitatively investigated to help explain the interactions occurring during the precipitation process.

EXPERIMENTAL PROCEDURES

Materials. The two anionic surfactants used in this study were sodium dodecyl sulfate (SDS) and sodium octyl benzene sulfonate (SOBS). Electrophoresis high-performance liquid chromatography (HPLC)-grade SDS was at least 99% pure and was obtained from Fisher Scientific (Pittsburgh, PA). It was further purified by recrystallization from water and then from methanol, followed by drying under a vacuum at approximately 30°C. SOBS was obtained from Aldrich (Milwaukee, WI) at a purity of 97%. SOBS was recrystallized first from methanol, and then from water. It was then rinsed with cold methanol and dried under a vacuum at approximately 30°C. Reagent-grade calcium chloride was obtained from Fisher Scientific and was used as received. Water was double-deionized.

Methods. (i) Precipitation phase boundaries. Precipitation phase boundaries for each surfactant are important to kinetic studies in order to quantify supersaturation. For each surfactant concentration studied, a series of solutions was made with varying $CaCl_2$ concentrations. Surfactant solu-

*To whom correspondence should be addressed at Department of Chemical Engineering, the University of Oklahoma, The Energy Center, 100 E. Boyd, Rm. T-335, Norman, OK 73019-0628.
E-mail: scamehor@ou.edu

tions can stay supersaturated for long periods of time (4,5) resulting in nonequilibrium apparent hardness tolerances. Therefore, the temperature of these solutions was first lowered to near 0°C for at least 24 h to force precipitation. The temperature was then held constant at 30°C for 4 d while gently shaking the samples daily to ensure equilibrium (6). For each series of solutions, some samples still contained crystals, whereas others became clear. The clear solutions were recorded as being below the precipitation phase boundary, and the turbid solutions were above the precipitation phase boundary. The solutions on the precipitation phase boundary contained the first amount of precipitate seen using a high-intensity beam of light.

Equilibrium supernatant concentrations for the individual surfactant components in the surfactant mixtures could be predicted at arbitrary initial conditions using a model by Stellner and Scamehorn (6,7). Experimental determination of a few points was done to verify the accuracy of the model for SDS/SOBS mixtures. Experimental determination of points along the precipitation phase boundary of the least-soluble surfactant in a mixture was found in the same way as for the pure surfactant hardness tolerance, using a high-intensity beam of light to detect the crystalline phase visually.

Experimental determination of a few points along the precipitation phase boundary for the more soluble surfactant was made by determining *via* conductivity the point where the more soluble surfactant was initially present in the crystals. Any solution still containing precipitate at equilibrium was filtered with a Whatman (Clifton, NJ) 3.0 μm pore size cellulose nitrate membrane filter, and each surfactant component concentration was analyzed with a Wescan conductivity detector *via* HPLC, using a reversed-phase silica column. The filtering was done quickly so that the solution remained isothermal. The absence of solids in the filtered supernatant was immediately confirmed with a high-intensity beam of light. The precipitate was washed with cold water to remove the mother liquor and dissolved in water. For the samples containing the more soluble surfactant, the initial solution concentration was considered to be inside the precipitation region for that surfactant. For solutions in which the more soluble surfactant was not detected in the precipitate, the initial solution concentration was considered to be outside the surfactant's precipitation phase boundary.

(ii) Calorimeter studies. A Tronac (Oreon, UT) model 458/558 calorimeter was used in isoperibol mode to measure the heat of reaction (which can be related to the amount of surfactant precipitated) as a function of time. Isoperibol calorimetry is a nearly adiabatic process. However, there is a small amount of heat transferred from the reaction vessel to the water bath and added to the reaction vessel by the stirrer and thermistors. Over short lengths of time, this heat leak can be modeled as a linear function of the reaction vessel temperature. The temperature of the water bath at 30°C can be maintained within ± 0.025°C using a Tronac PTC-41 temperature controller. The rates of precipitation of SDS/SOBS mixtures with calcium were measured. Total concentrations of 0.0025, 0.0096, 0.0192, 0.0288, and 0.0750 M were studied with SDS/SOBS mole ratios of 0:1, 0.2:0.8, 0.4:0.6, 0.6:0.4, 0.8:0.2, and 1:0. Approximately 48 g of surfactant solution was placed in the reaction vessel, and approximately 2 g of 0.25 M calcium chloride solution was injected into a soft glass ampoule which was then sealed with a Microflame (Foxboro, MA) butane torch and placed in the ampoule holder/stirrer. The system was then allowed to equilibrate to the water bath temperature. The ampoule could then be broken with the hammer to allow nearly instantaneous mixing of the reactants, which were being stirred vigorously.

(iii) Rate of precipitation. When an anionic surfactant solution is mixed with a counterion, the apparent experimental heat of reaction is the total heat released from the precipitation reaction, dilution of the ampoule contents, dilution of the reaction vessel contents, breaking of the ampoule, and in some cases, micelle formation and dissociation. Additional experiments must be done to determine these extraneous heats. The heat of breaking the ampoule was measured by breaking an ampoule containing water into the reaction vessel containing water. Heat of dilution of the ampoule solution was measured by breaking an ampoule containing a solution of $CaCl_2$ into water, and heat of dilution of the reaction vessel solution was measured by breaking water into the appropriate reaction vessel solution. Heat of micellization was measured by breaking an ampoule containing a concentrated $CaCl_2$ solution into a surfactant solution that was above the CMC, but outside the precipitation region. This resulted in the formation of additional micelles without precipitation. The decrease in the CMC upon addition of a counterion was calculated using a model developed by Stellner and Scamehorn (7). A Microscribe 450 (San Jose, CA) chart recorder was used to plot the temperature difference between the reaction vessel and the water bath, in voltage, vs. time. For each run, the average heat capacity, C_p, was obtained by adding a known amount of heat for a known amount of time before and after the reaction. Then, by using this heat capacity, the overall heat produced during a reaction, Q_T, could be obtained:

$$Q_T = C_p \Delta T \qquad [1]$$

where ΔT is the total temperature change (proportional to the voltage in mV), during the reaction minus the heat leak discussed in the previous section.

For systems that start above the CMC, demicellization occurs as the precipitation reaction proceeds due to an equilibrium shift from the micelles to the monomers. The heat associated with this process should be subtracted from the heat of reaction as a function of time. The concentration of surfactant as micelles in solution can be found at each point during a reaction using the same model by Stellner and Scamehorn (7) along with a model of the precipitation reaction pathway (8–10). The heat due only to precipitation at each point along the reaction pathway can thus be separated from all of the extraneous heats associated with a calorimeter run.

(iv) Coprecipitation. To examine whether a surfactant that is not supersaturated incorporates into the crystals of a precipitating surfactant, we mixed supersaturated concentrations of SDS at various concentrations and an undersaturated concentration of SOBS (2.5×10^{-4} M SOBS) in the calorimeter. The experiments were then repeated with the roles of SDS and SOBS reversed. The supersaturated solutions contained 0.020, 0.010, 0.0025, 0.0010, and 0.0006 M surfactant with 0.010 M $CaCl_2$. The solutions were filtered immediately after the precipitation reaction was complete with a Whatman 3.0 m pore size cellulose nitrate membrane filter, and concentrations were measured with a Wescan conductivity detector *via* HPLC using a reversed- phase silica column. Solutions containing 2.5×10^{-4} M SDS and 2.5×10^{-4} M SOBS with 0.010 M $CaCl_2$ were stirred for over 30 min at 30°C to ensure that these solutions were in fact nonprecipitating.

(v) Surfactant adsorption on precipitate. Adsorption of a surfactant which is not precipitating onto the surface of crystals of the dissimilar surfactant was determined by the solution depletion method. The concentration change of the nonprecipitating surfactant was measured in a solution upon immersion of crystals of the precipitating surfactant and completion of equilibration. Specifically, solutions of 0.02 M SDS or 0.02 M SOBS were precipitated using 0.01 M $CaCl_2$. The precipitated solutions were then filtered, and the precipitate was dried and weighed. Solutions of each surfactant that would not form precipitate at equilibrium were made and placed in a constant-temperature water bath at 30°C; both SDS and SOBS solutions were made with surfactant concentrations of 1.0×10^{-5}, 5.0×10^{-5}, 1.0×10^{-4}, 1.5×10^{-4}, 2.0×10^{-4}, and 2.5×10^{-4} M. Dried and weighed $Ca(DS)_2$ precipitate (where DS represents the dodecyl sulfate anion) was added to each dilute solution of SOBS, and vice versa. The solutions were then held at 30°C for 4 d, which is sufficient to ensure equilibrium even for porous solids with high surface area (11). The solutions were then filtered with a Whatman 3.0 μm pore size cellulose nitrate membrane filter. The filtering was done quickly so that the solution remained almost isothermal. The filter cake was rinsed with cold water to remove the mother liquor, and dissolved in water. A reversed-phase silica column in HPLC with a Wescan conductivity detector was then used to measure surfactant concentrations.

(vi) Precipitate composition. Precipitate compositions were obtained at various points during the precipitation reaction for a range of SDS/SOBS mixtures. This study was done to determine whether any correlation existed between which surfactants precipitated at the various points during the precipitation reaction and the precipitation behavior at these points. A series of 48-g solutions containing 0.0196 M surfactant were precipitated by the addition of 2 mL of 0.25 M $CaCl_2$. The solution being precipitated was stirred vigorously by a submersible stir plate in a 30°C water bath. Each reaction was stopped at different times by quickly filtering *via* a Whatman 1.0 μm pore size cellulose nitrate filter, and then the first portion of the filtered solution was thrown out. The time required to obtain a filtered sample was noted. The filtered solutions were diluted and the concentrations measured with an Alltech 320 conductivity detector (Deerfield, IL) *via* a Shimadzu LC-10AD HPLC (Tokyo, Japan) using a reversed-phase silica column.

(vi) Crystal habits. Image analysis was used to determine any change in crystal habit as SDS and SOBS were mixed in supersaturated solutions. Bottles containing 48 mL of different surfactant mixtures were placed on a submersible stirrer in a constant-temperature water bath. As the surfactant solution was vigorously stirred, 2 mL of $CaCl_2$ was quickly pipetted into the surfactant solution. Each experiment was allowed to continue for either 4 min or 1 wk so that the crystals could be analyzed just after precipitation and after ripening. At the end of the time allotment, a sample was removed, placed on a slide, and a 40× picture was saved through the image analysis *via* Optimas software. The solutions studied were 0.075 M SOBS with 0.010 M $CaCl_2$, 0.010 M SDS with 0.008 M $CaCl_2$, and the mixtures 0.010 M SDS/0.002 M SOBS, and 0.01 M SDS/0.004 M SOBS, each with 0.008 M $CaCl_2$.

RESULTS AND DISCUSSION

Precipitation phase boundaries. Along a precipitation phase boundary, an infinitesimal amount of precipitate is present, which normally consists of only one ionic surfactant. Precipitation occurs below the CMC when the solubility product relationship for the least soluble surfactant is reached. The solubility product relationship for a surfactant anion with calcium below the CMC is described in Equation 2:

$$K_{SP} = [S^-]^2 [Ca^{2+}] f_S^2 f_{Ca} \quad [2]$$

where K_{SP} is the activity-based solubility product, $[S^-]$ is the total surfactant concentration of the precipitating anionic surfactant, and $[Ca^{2+}]$ is the total calcium concentration in solution. Total concentrations used are below the CMC since all of the surfactant is in its monomer form. The parameters f_S and f_{Ca} are the activity coefficients of the surfactant and calcium, respectively. Along the precipitation phase boundary and above the CMC, a simultaneous equilibrium exists between the precipitating surfactant as monomer, in micelles, and in precipitate. Precipitation occurs above the CMC when the monomeric concentration of the least soluble ionic surfactant, along with the unbound counterion concentration, equals the surfactant's solubility product (12). The solubility product relationship that describes surfactant precipitation above the CMC is shown in Equation 3:

$$K_{SP} = ([S^-]_{mon})^2 [Ca^{2+}]_{un} f_S^2 f_{Ca} \quad [3]$$

where $[S^-]_{mon}$ is the monomeric concentration of the precipitating surfactant and $[Ca^{2+}]_{un}$ is the unbound calcium concentration (calcium not bound to the micelles). The activity coefficients for insertion into Equations 2 and 3 are found using an extended Debye-Huckel expression (13):

$$\log f_i = -A\,(z_i)^2\, I^{0.5}/(1 + B\,a_i\, I^{0.5}) - 0.3\, I \qquad [4]$$

The constants A and B are dependent on the solvent and the temperature of solution. At 30°C, A has a value of 0.5139 and B has a value of 0.3297×10^8 (14). The parameter z_i is the ion valence and is equal to −1 for either anionic surfactant and +2 for calcium. The parameter a_i is an empirical value based on the diameter of the ion, and is equal to 6×10^{-8} cm^{-1} for calcium (14) and is estimated as 7×10^{-8} cm^{-1} for SDS and SOBS (6,14,15). The parameter I is the ionic strength of the solution. For this study, the ionic strength is given as

$$I = \Sigma\, 0.5\, c_i\, (z_i)^2 = [\mathrm{SDS}] + [\mathrm{SOBS}] + 3[\mathrm{CaCl_2}] \qquad [5]$$

where c_i is the total concentration of ion i in solution, [SDS] and [SOBS] are the total concentrations of SDS and SOBS in solution, and [$CaCl_2$] is the total $CaCl_2$ concentration in solution.

Below the CMC, as the anionic surfactant concentration increases, the amount of calcium required for precipitation to occur decreases, as dictated by Equation 2. The effect of micelle formation on surfactant precipitation is an increase in the concentration of calcium required for precipitation to occur. When micelles form, calcium ions bind to the micelles, reducing the amount of unbound calcium available for precipitation. As more surfactant is added to the system, the additional surfactant tends to form more micelles. The formation of more micelles reduces $[Ca^{2+}]_{un}$ even further. Therefore, a minimum in the precipitation phase boundary occurs at the CMC.

When two surfactants of similar structure and charge are mixed together, ideal mixed micelles form (12,16). Scheme 1 shows a micelle-monomer-precipitate equilibrium diagram for a mixture of two anionic surfactants in the presence of calcium. There are also sodium ions in solution due to the dissociation of the surfactant salt; these are not shown in Scheme 1 for clarity. Sodium does not precipitate the anionic surfactants studied at the concentration levels present in this paper due to a much larger K_{SP} with these surfactants than the calcium salt. The hardness tolerance of a mixture containing more than one anionic surfactant is obtained when the solubility product of the least soluble surfactant is reached (12,16). Mixed precipitate is usually not seen along the precipitation phase boundary of mixed anionic surfactants unless the K_{SP} values of the two surfactants are very similar (17). As a consequence of both surfactants participating in mixed micelle formation and only one surfactant participating in precipitation (at the hardness tolerance where an infinitesimal amount of solid is present) as the precipitating surfactant is mixed with another anionic surfactant, the precipitating surfactant is diluted in the micellar phase. This shifts the equilibrium toward the micelles and causes precipitation of that surfactant to be more difficult, and so hardness tolerance increases.

A general model has been developed that can predict the hardness tolerance of an anionic surfactant (6,7) using the pseudo-phase separation theory (18,19) to describe the micelle-monomer equilibrium that occurs in micellar solutions. This model can be used to predict the hardness tolerance of a mixture as well as the monomer and micellar concentrations of each component in the system. The hardness tolerance of the mixture is defined as the minimum calcium concentration at which surfactant precipitates at equilibrium. This would correspond to the calcium concentration at which the K_{SP} of one of the surfactants is first satisfied. By using the solubility product relationship, the hardness tolerance model, and material balances, the amount of calcium required initially in the solution to subsequently satisfy the solubility product of the surfactant component that precipitates with more difficulty can be calculated.

The theoretical precipitation phase boundaries for the surfactant components in several SDS/SOBS mixtures are shown in Figures 1 and 2, along with some experimental re-

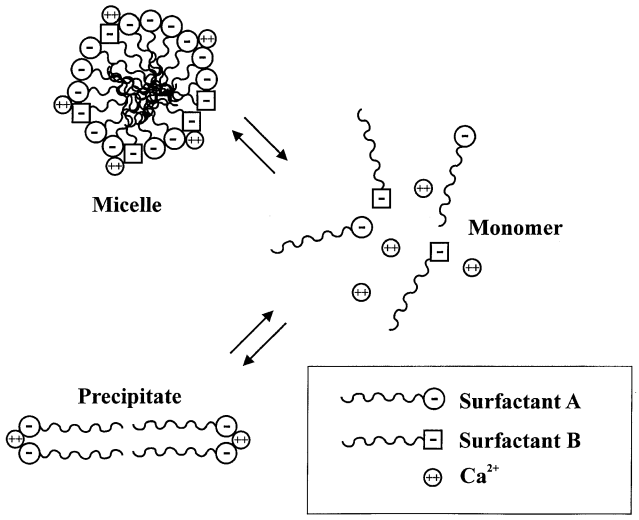

SCHEME 1

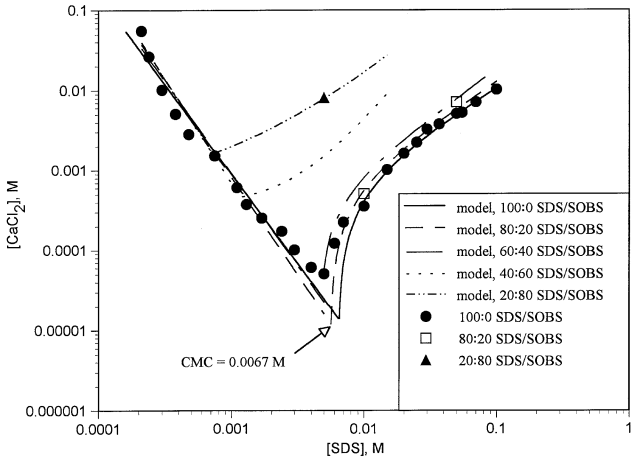

FIG. 1. Theoretical precipitation phase boundaries for sodium dodecyl sulfate (SDS) in various SDS/sodium octyl benzene sulfonate (SOBS) mixtures as well as comparison with experimental hardness tolerance points, both at 30°C. CMC, critical micelle concentration.

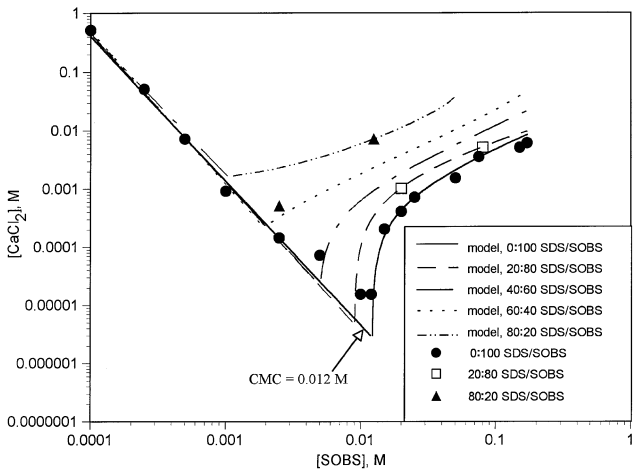

FIG. 2. Theoretical precipitation phase boundaries for SOBS in various SDS/SOBS mixtures as well as comparison with experimental hardness tolerance points, both at 30°C. For abbreviations see Figure 1.

sults for confirmation of the model's accuracy. The model fits the data for pure SDS (6) and pure SOBS quite well as we have seen before. The minimum in the hardness tolerance in Figures 1 and 2 corresponds to the CMC values of SDS and SOBS, respectively; the surfactant concentration corresponding to the minimum in the SDS hardness tolerance is 0.0067 M (6) and in the SOBS hardness tolerance is 0.012 M. These values are consistent with the CMC values obtained from surface tension measurements: 0.0072 M for SDS and 0.012 M for SOBS (20). On the left side of each precipitation phase boundary, the surfactant is present as monomer, and on the right side, the surfactant is present as monomer and in micelles. For each mixture, there is a precipitation phase boundary in Figures 1 and 2 that describes the minimum calcium concentration in solution at which that component would precipitate in the mixture. Above the minimum hardness tolerance, as SDS is mixed with SOBS from 100:0 to 60:40 SDS/SOBS, the precipitation phase boundary for SDS slightly increases. At 40:60 and then 20:80 SDS/SOBS, the right side of the precipitation phase boundary for SDS dramatically increases. This same trend is seen for the 60:40 and 80:20 SDS/SOBS solutions at the SOBS precipitation phase boundaries. Below the mixture CMC, no significant change in the precipitation phase boundary is seen as the two surfactants are mixed. This shows that the effect of mixed micelles causes the large increase in the hardness tolerances for each surfactant. According to theory, SDS should precipitate at lower $CaCl_2$ concentrations at 80:20 and 60:40 SDS/SOBS, and SOBS should precipitate at lower $CaCl_2$ concentrations at 20:80 and 40:60 SDS/SOBS. Hence, the hardness tolerance of the surfactant mixture corresponds to different surfactants precipitating at different mixture compositions. The individual surfactant component hardness tolerances can be obtained theoretically even when this surfactant is not the least soluble (there is already precipitate in the system due to precipitation of another surfactant component with calcium). The hardness tolerances for SDS at 40:60 and 20:80 SDS/SOBS are the predicted hardness tolerances for SDS in the presence of $Ca(OBS)_2$ precipitate (where OBS = octyl benzene sulfonate anion). The hardness tolerances for SOBS at 60:40 and 80:20 SDS/SOBS are the predicted hardness tolerances for SOBS in the presence of $Ca(DS)_2$ precipitate (where DS = dodecyl sufate anion).

Several experimental hardness tolerance points above the CMC are shown in Figures 1 and 2 for comparison with the theoretical curve. For 20:80 SDS/SOBS, SOBS has a lower hardness tolerance and therefore $Ca(OBS)_2$ theoretically precipitates from solution before $Ca(DS)_2$. For the precipitation of $Ca(OBS)_2$ from a 20:80 SDS/SOBS solution, at 0.025 and 0.1 M total surfactant concentration, the theory and experimental hardness tolerance points agree. The experimental hardness tolerance of SDS from 20:80 SDS/SOBS and 0.025 M total surfactant also matches the predicted points. The onset of precipitation of $Ca(DS)_2$ from 20:80 SDS/SOBS and 0.1 M surfactant was not obtained owing to SDS showing up on the HPLC chart as a shoulder peak to the much larger SOBS peak, making the exact determination of this point difficult. For 80:20 SDS/SOBS, SDS has a lower hardness tolerance and therefore $Ca(DS)_2$ theoretically precipitates from solution before $Ca(OBS)_2$. For the precipitation of SDS from 0.0125 and 0.0625 M surfactant and 80:20 SDS/SOBS, the data match the theory reasonably well. However, for the precipitation of SOBS with calcium from these same solutions, the experimental hardness tolerance is less than the theoretical prediction. The SOBS component is detected in the precipitate for these mixtures at the lowest calcium concentration where there is enough precipitate to allow separation and analysis. The presence of any $Ca(DS)_2$ precipitate results in the presence of OBS^- in the precipitate. However, the precipitation of $Ca(OBS)_2$ does not result in the presence of DS^- in the precipitate. In fact, DS^- is not detectable in the precipitate until the solubility product of SDS and calcium has been reached. A possible explanation for this behavior is that OBS^- adsorbs onto the $Ca(DS)_2$ crystals, accounting for its presence in the solid phase.

Adsorption studies. The adsorption of OBS^- onto precipitating $Ca(DS)_2$ crystals was determined qualitatively. An adsorption isotherm could not be obtained since the initial adsorbing surfactant concentration would lie in the middle of the precipitating region. This would always raise the question of whether all of the adsorbing surfactant and precipitate were dissolved at equilibrium. Also, the precipitate weight can change due to partial dissolution. Therefore, the question of whether significant adsorption occurs was addressed, but the amount could not be quantified. Significant amounts of OBS^- were detected in the $Ca(DS)_2$ crystals after 4 d for every sample studied. However, there was no evidence of any DS^- in the $Ca(OBS)_2$ crystals after the same time span. This result gives evidence for the ability of OBS^- to adsorb onto the $Ca(DS)_2$ crystals and gives a possible explanation for the deviation of the experimental points on the SOBS precipitation phase boundary for the 80:20 SDS/SOBS system.

Determination of supersaturation and reaction pathways. A solution that contains surfactant and calcium concentrations lying inside the precipitation phase boundary is supersaturated. Supersaturation is a measure of the excess concentration of the reactants above the equilibrium solubility concentrations (21–23) and has been defined mathematically (1).

In a solution containing two anionic surfactants, the supersaturation ratio for each surfactant can be calculated separately. Using a supersaturation ratio that considers only the monomer surfactant and unbound calcium concentrations allows the effect of micelles to be accounted for. Thus, above the CMC, as a surfactant is diluted due to mixing with another surfactant, the supersaturation ratio for that surfactant will generally decrease.

Figures 3 and 4 show examples of reaction pathways of SDS with calcium compared with the SDS component precipitation phase boundaries for 80:20 and 20:80 SDS/SOBS, respectively. Similar comparisons for the precipitation of $Ca(OBS)_2$ from SDS/SOBS mixtures can also be made (20). The point where a reaction pathway crosses the precipitation phase boundary is the theoretical equilibrium supernatant concentration for that reaction. Any reaction pathway that begins outside of the precipitation phase boundary represents a solution where $Ca(DS)_2$ should not precipitate. As the precipitation region decreases for SDS as the SDS/SOBS ratio decreases (in the order 100:0, 80:20, 60:40, 40:60, and 20:80), the supersaturation ratio for SDS with calcium decreases. However, as the supersaturation ratio for SDS decreases, the supersaturation ratio for SOBS increases.

Effect of impurities on crystallization. Additional components in a solution can affect both the growth rate and crystal habit of a precipitating species (24,25). The supersaturation ratio can be changed owing to the effect of impurities on the solubility of the precipitating species (24,26). Selective adsorption of a constituent can change the crystal habit by retarding the outward growth of certain planes (27). Adsorption can also affect surface nucleation as well as overgrowths, incomplete planes, steps, and dislocations (27,28).

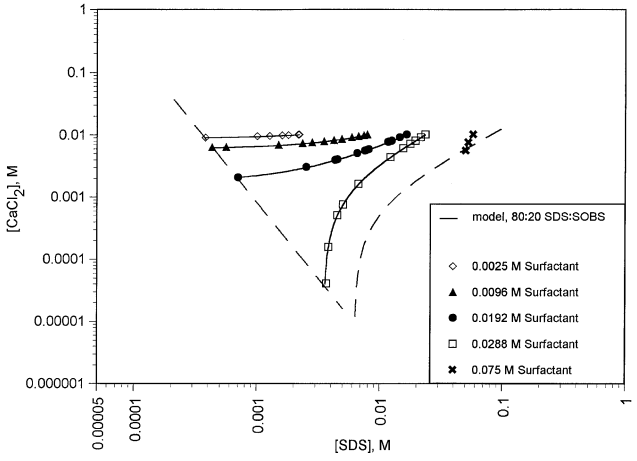

FIG. 3. Comparison between SDS-$CaCl_2$ precipitation reaction pathways for various total surfactant concentrations and 80:20 SDS/SOBS solution and the precipitation phase boundary for SDS for the 80:20 SDS/SOBS system at 30°C. For abbreviations see Figure 1.

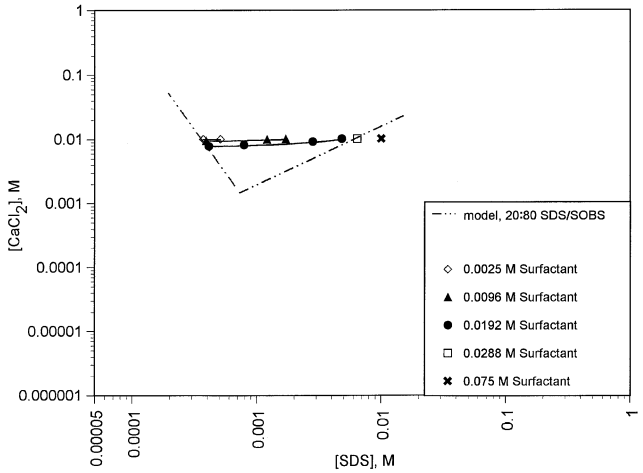

FIG. 4. Comparison between SDS-$CaCl_2$ precipitation reaction pathways for various total surfactant concentrations and 20:80 SDS/SOBS solution and the precipitation phase boundary for SDS for the 20:80 SDS/SOBS system at 30°C. For abbreviations see Figure 1.

Epitaxial growth is the oriented growth of a crystalline phase on the surface of another crystalline phase and depends on the lattice structure (28,29). If both species are supersaturated, epitaxial growth can affect the overall time for precipitation to eventuate. An increase in the overall time for precipitation to occur could take place if epitaxial growth covers a screw dislocation.

Coprecipitation can occur when an impurity or microcomponent is present in solution, resulting in inclusion and/or the formation of a solid solution. A solid solution occurs when trace ions or molecules are incorporated into the host lattice during precipitation. The tendency for a solid solution to form depends on whether the macrocomponent and the microcomponent have similar ionic radii and the same charge (21). In surfactant systems, it would also be important that the two components have similar overall structures. Inclusion (26), sometimes called occlusion, is the entrapment of impurities during precipitation. This can occur due to adsorption, chemical reaction, or entrapment of the mother liquor in pockets as imperfect layers are formed. In each of these cases (except when a chemical reaction has occurred), the impurity is free to diffuse through the solid phase and even to separate during ripening (21,30). In most situations where coprecipitation occurs, a combination of these phenomena exists (30).

Precipitation kinetics for SDS/SOBS mixtures with calcium. Figures 5–9 depict the extent of precipitation curves as a function of time for 0.075, 0.0288, 0.0192, 0.0096, and 0.0025 M total surfactant concentration for the entire range of SDS/SOBS mole ratios. Figure 5 shows the extent of precipitation with time of solutions containing 0.075 M surfactant and 0.01 M $CaCl_2$. Even though 0.075 M SDS is inside the precipitation phase boundary, and a small amount of

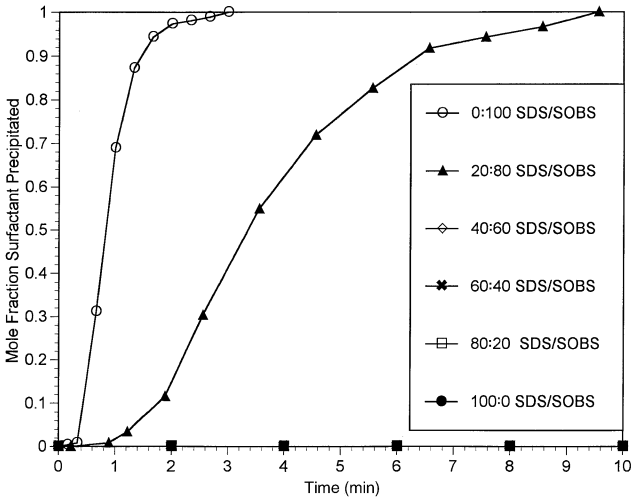

FIG. 5. Precipitation rate curves for 0.075 M total surfactant concentration and varying SDS/SOBS mole fractions with 0.01 M $CaCl_2$ at 30°C. For abbreviations see Figure 1.

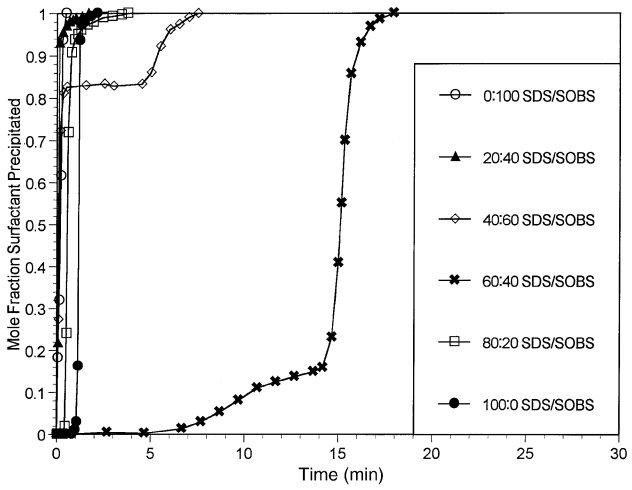

FIG. 7. Precipitation rate curves for 0.0192 M total surfactant concentration and varying SDS/SOBS mole fractions with 0.01 M $CaCl_2$ at 30°C. For abbreviations see Figure 1.

precipitate is seen at the end of the experiment, the heat released during the reaction is too small to measure with the technique used here. This result is most likely due to the SDS concentration being very close to the precipitation phase boundary. The 80:20, 60:40, and 40:60 SDS/SOBS solutions did not contain any visible precipitate at the end of the calorimeter runs. In general for the systems studied, as SDS and SOBS are mixed, the overall time for precipitation to occur is increased, with 60:40 SDS/SOBS requiring the longest time. In Figure 6, the precipitation reaction for 60:40 SDS/SOBS takes approximately 35 min. This curve is not shown beyond 4.5 min to permit easier comparisons to the other data. The initial supersaturation ratios for each reaction are given in Tables 1–5, corresponding with Figures 5–9. Also, the percentages of SDS and SOBS in the precipitate at the end of the reaction are given in Tables 1, 2, 4, and 5. In general, as a surfactant is diluted as it is mixed with another surfactant, the initial supersaturation ratio for that surfactant decreases and the final fraction of that surfactant in the precipitate decreases.

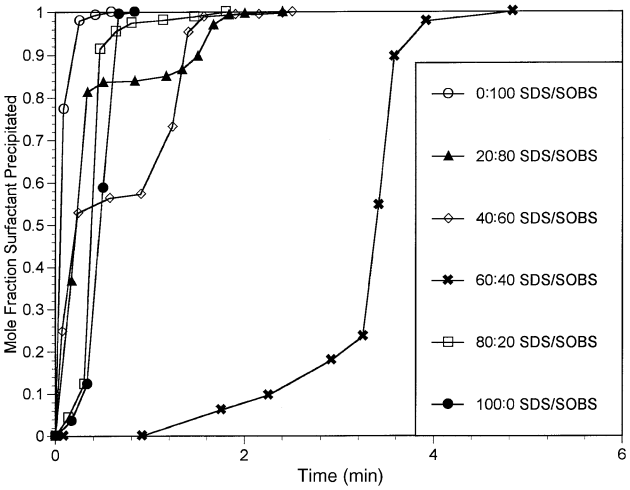

FIG. 8. Precipitation rate curves for 0.0096 M total surfactant concentration and varying SDS/SOBS mole fractions with 0.01 M $CaCl_2$ at 30°C. For abbreviations see Figure 1.

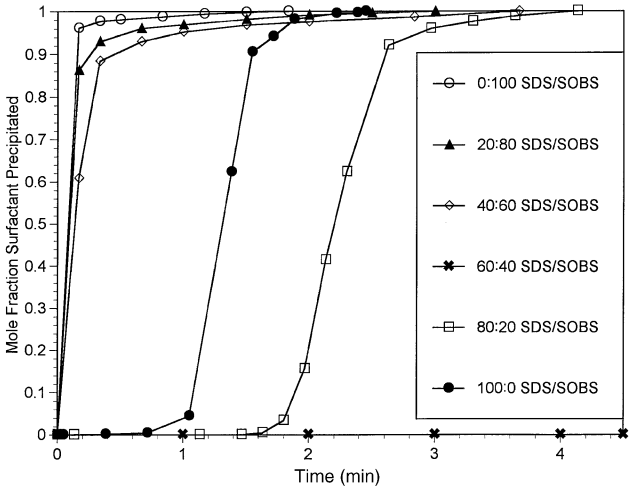

FIG. 6. Precipitation rate curves for 0.0288 M total surfactant concentration and varying SDS/SOBS mole fractions with 0.01 M $CaCl_2$ at 30°C. For abbreviations see Figure 1.

For each 80:20 SDS/SOBS precipitation reaction where the precipitation composition was determined, DS^- and OBS^- were both present in the precipitate. However, our experimental technique does not generate individual extent of precipitation curves for the separate precipitation of the two surfactants. The time for precipitation to occur as the SDS/SOBS mole ratio changed from 100:0 to 80:20 and 60:40 increased along with the supersaturation ratio of SDS. For the change in SDS/SOBS mole ratios from 60:40 to 80:20, the supersaturation ratio for SOBS decreased, in-

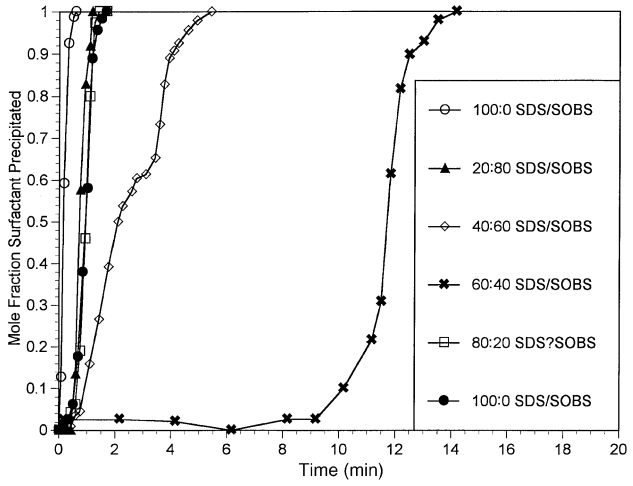

FIG. 9. Precipitation rate curves for 0.0025 M total surfactant concentration and varying SDS/SOBS mole fractions with 0.01 M $CaCl_2$ at 30°C. For abbreviations see Figure 1.

dicating that the independent precipitation of SOBS with calcium should decrease. An explanation for this behavior is that OBS^- is being included into the $Ca(DS)_2$ crystal as it forms (by adsorption and possibly entrapment of the mother liquor). If the supersaturation of SOBS is satiated by this interaction, a separate reaction rate would not occur for the precipitation of $Ca(OBS)_2$.

The overall time for precipitation to occur for 60:40 SDS/SOBS in each case is much longer than would be expected from comparing the degree of decrease in supersaturation ratios as each surfactant is diluted to this point, from single surfactant precipitation rates. For 0.0288, 0.0096, and 0.0025 M surfactant, both surfactants are present in the precipitate at the end of the calorimeter run, even though a smooth precipitation kinetics curve is seen. However, these interactions do not explain the drastic increase in time seen only for the precipitation of 60:40 SDS/SOBS.

An initial increase in the extent of reaction followed by a leveling off and a second increase is seen for 40:60 SDS/SOBS, and 0.0096, 0.0192, and 0.0025 M surfactant. This stepwise precipitation behavior is also seen for 20:80 SDS/SOBS and 0.0096 M surfactant. Both surfactants are present in the precipitate at the end of the runs where the concentration was measured (Tables 1, 2, 4, and 5). To help explain the precipitation behavior of these solutions, the precipitate for 40:60 SDS/SOBS and 0.0092 M surfactant was analyzed at various times during the reaction to determine the relative precipitation of each surfactant component as the reaction progressed. The resulting concentrations related to the extent of reaction are shown in Figure

TABLE 1
Comparison of Initial Supersaturation Ratios (S_o) with Precipitate SDS/SOBS Molar Ratios for Various 0.075 M SDS/SOBS Mixtures Precipitated with 0.01 M $CaCl_2$ at 30°C[a]

SDS/SOBS	S_o of SDS	S_o of SOBS	SDS/SOBS in precipitate
0.0:100	0.0	5.44	0.0:100.0
20:40	0.84	4.16	0.0:100.0
40:60	1.36	3.49	—
60:80	1.73	2.59	—
80:20	1.93	1.50	—
100:0	1.98	0.00	—

[a]Abbreviations: SDS, sodium dodecyl sulfate; SOBS, sodium octyl benzene sulfonate.

TABLE 2
Comparison of Initial Supersaturation Ratios (S_o) with Precipitate SDS/SOBS Molar Ratios for Various 0.0288 M SDS/SOBS Mixtures Precipitated with 0.01 M $CaCl_2$ at 30°C[a]

SDS/SOBS	S_o of SDS	S_o of SOBS	SDS/SOBS in precipitate
0.0:100	0.00	8.90	0.0:100.0
20:80	1.76	7.42	0.0:100.0
40:60	2.64	5.84	0.0:100.0
60:40	3.38	4.37	1.8:98.2
80:20	3.91	2.65	96.1:3.9
100:0	4.31	0.00	100.0:0.0

[a]For abbreviations see Table 1.

TABLE 3
Comparison of Initial Supersaturation Ratios (S_o) for Various 0.0192 M SDS/SOBS Mixtures Precipitated with 0.01 M $CaCl_2$ at 30°C[a]

SDS/SOBS	S_o of SDS	S_o of SOBS
0.0:100	0.00	10.11
20:80	2.20	8.17
40:60	3.22	6.48
60:40	4.29	4.96
80:20	4.76	2.89
100:0	5.42	0.00

[a]For abbreviations see Table 1.

TABLE 4
Comparison of Initial Supersaturation Ratios (S_o) with Precipitate SDS/SOBS Molar Ratios for Various 0.0096 M SDS/SOBS Mixtures Precipitated with 0.01 M $CaCl_2$ at 30°C[a]

SDS/SOBS	S_o of SDS	S_o of SOBS	SDS/SOBS in precipitate
0:100	0.00	9.25	0.0:100.0
20:80	3.01	8.01	6.8:93.2
40:60	4.74	6.56	22.0:78.0
60:40	5.71	4.82	11.8:88.2
80:20	6.45	2.93	81.1:18.9
100:0	7.07	0.00	100.0:0.0

[a]For abbreviations see Table 1.

TABLE 5
Comparison of Initial Supersaturation Ratios (S_o) with Precipitate SDS/SOBS Molar Ratios for Various 0.0025 M SDS/SOBS Mixtures Precipitated with 0.01 M $CaCl_2$ at 30°C[a]

SDS/SOBS	S_o of SDS	S_o of SOBS	SDS/SOBS in precipitate
0:100	0.00	3.86	0.0:100.0
20:80	1.25	3.33	0.0:100.0
40:60	1.97	2.73	21.8:78.2
60:40	2.57	2.07	64.8:35.2
80:20	3.12	1.31	95.9:4.1
100:0	3.65	0.00	100.0:0.0

[a]For abbreviations see Table 1.

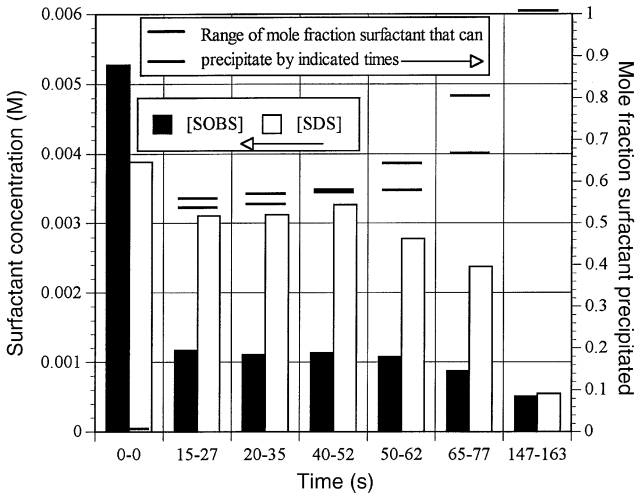

FIG. 10. Concentration vs. time at 30°C for 0.0092 M surfactant, 40:60 SDS/SOBS, and 0.01 M $CaCl_2$ as related to the extent of precipitation during each time segment. For abbreviations see Figure 1.

TABLE 6
Nonequilibrium Crystal Compositions, Precipitated from Various Supersaturated Concentrations of SDS and SOBS in the Presence of Dilute Surfactant[a]

[SDS]	[SOBS]	SDS/SOBS in precipitate
0.00025	0.02	0.0:100.0
0.00025	0.01	18.7:81.3
0.00025	0.0025	9.5:90.5
0.00025	0.0006	8.7:91.3
0.00025	0.0	—
0.02	0.00025	97.7:2.2
0.01	0.00025	87.2:12.8
0.0025	0.00025	96.1:3.9
0.001	0.00025	97.9:2.1
0.0006	0.00025	98.1:1.9
0.0	0.00025	—

[a]For abbreviations see Table 1.

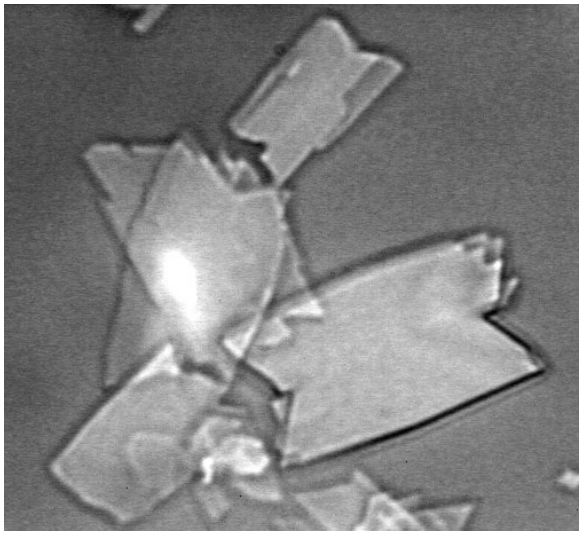

FIG. 11. Image analysis picture of $Ca(OBS)_2$ crystals at 40× precipitated from a 0.075 M SOBS/0.010 M $CaCl_2$ solution; taken 4 min after mixing at 30°C. For abbreviations see Figure 1.

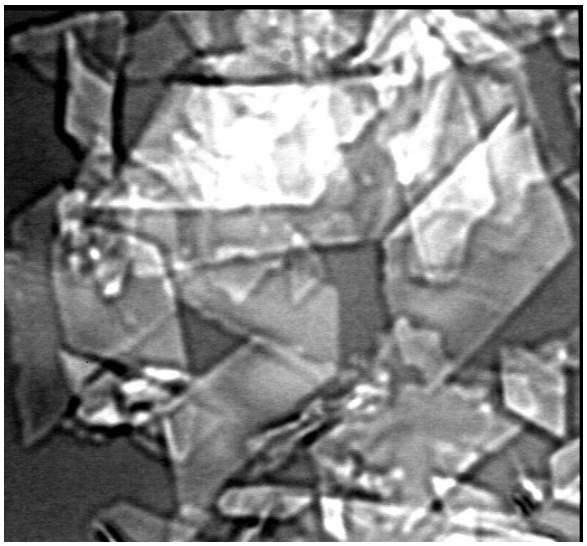

FIG. 12. Image analysis picture of $Ca(DS)_2$ crystals at 40× precipitated from a 0.010 M SDS/0.008 M $CaCl_2$ solution; taken 4 min after mixing at 30°C. For abbreviations see Figure 1.

10. The time spans for each measurement are the result of experimental restraints. During the first reaction step, the SOBS concentration drops dramatically. However, there is also a decrease in the SDS concentration. There is then an induction period during which both concentrations remain relatively constant. During the second reaction step, the SDS concentration drops more drastically than does the SOBS concentration. Evidence has already been presented to show that both SDS and SOBS can be present in the solid phase. This seems to be occurring in this 40:60 SDS/SOBS reaction as well. During the first reaction step, $Ca(OBS)_2$ is

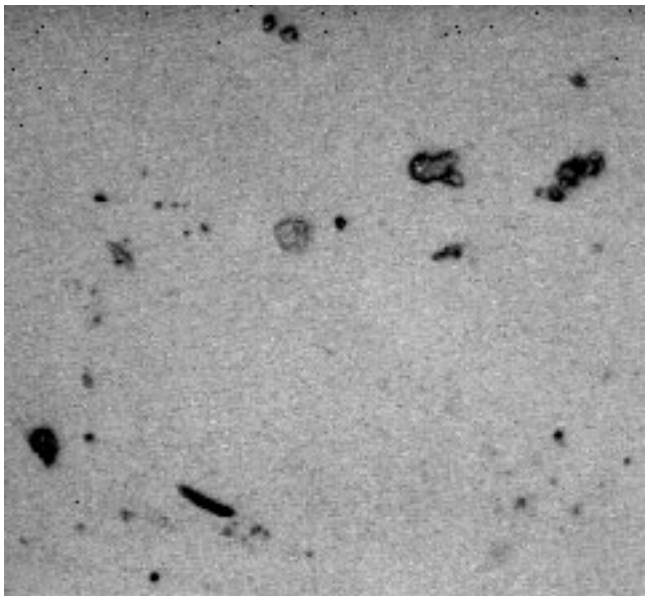

FIG. 13. Image analysis picture of crystals at 40× precipitated from a 0.012 M surfactant solution containing 83:17 SDS/SOBS and 0.008 M $CaCl_2$; taken 4 min after mixing at 30°C. For abbreviations see Figure 1.

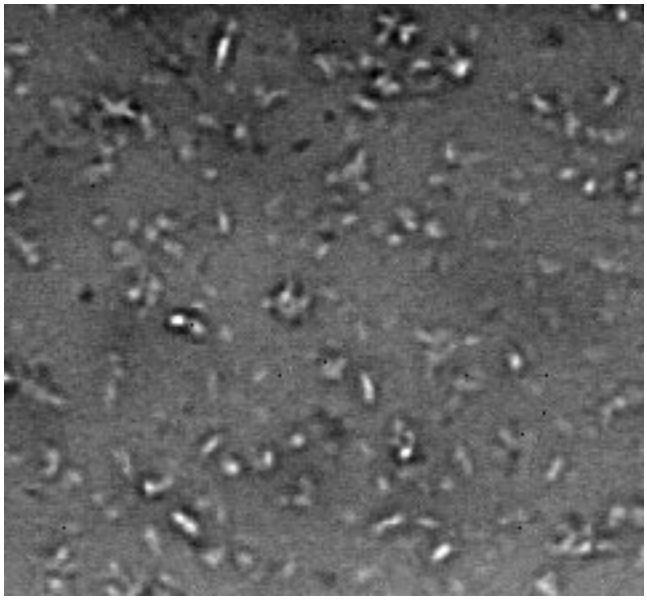

FIG. 14. Image analysis picture of crystals at 40× precipitated from a 0.014 M surfactant solution containing 71:29 SDS/SOBS and 0.008 M $CaCl_2$; taken 4 min after mixing at 30°C. For abbreviations see Figure 1.

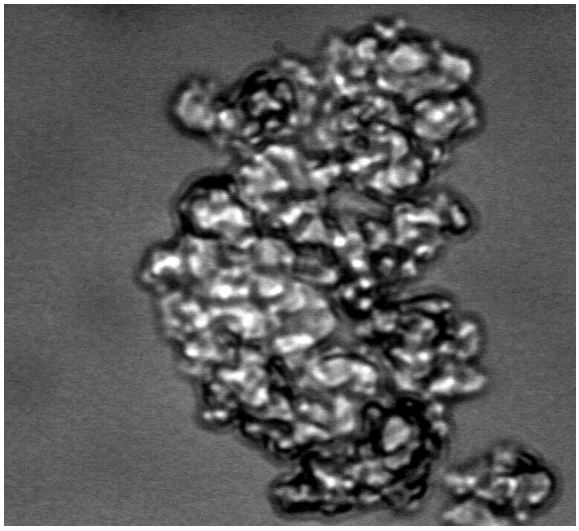

FIG. 16. Image analysis picture of $Ca(DS)_2$ crystals at 40× precipitated from a 0.010 M SDS/0.008 M $CaCl_2$ solution; taken after 1 wk at 30°C. For abbreviations see Figure 1.

the major precipitating component. The decrease in SDS concentration during this reaction step could likely be due to inclusion into the $Ca(OBS)_2$ crystals. The major precipitating component in the second reaction step is $Ca(DS)_2$. The induction time then can be considered the continuation of the total induction time required for the precipitation of $Ca(DS)_2$ from this solution. A further investigation into the precipitation of anionic surfactant mixtures has been done using atomic force microscopy (20).

Nonequilibrium crystal compositions. Table 6 shows the crystal compositions during crystallization prior to attainment of equilibrium for precipitation of an anionic surfactant in the presence of a different dilute anionic surfactant. In this experiment, the crystals were filtered from the solution at a specific time during the precipitation reaction. Since precipitation from direct mixing inherently results in broad crystal size distributions, and since the supersaturation ratio is being altered, it is not certain whether each sample contained the same crystal surface areas or morphologies. However, whether coprecipitation occurs can be unambiguously determined. Table 6 shows that DS^- is found in the nonequilibrium precipitate of $Ca(OBS)_2$ and OBS^- is found in both the nonequilibrium and equilibrium precipitate of $Ca(DS)_2$. DS^- was not found in the $Ca(OBS)_2$ crystals at equilibrium. The two surfactants have dissimilar structures; SOBS has a benzene ring in an eight-carbon chain and a

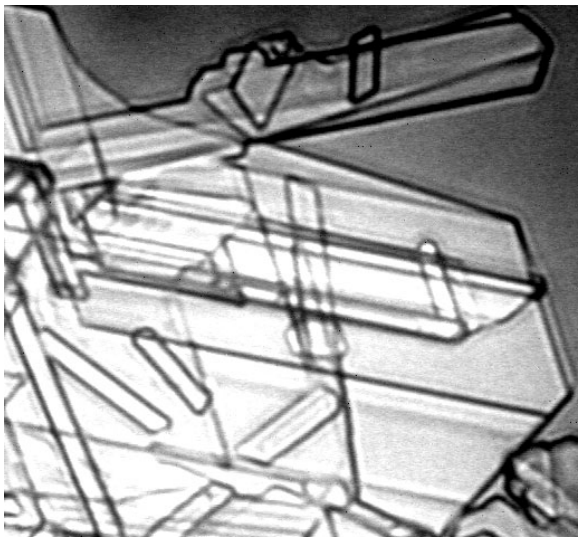

FIG. 15. Image analysis picture of $Ca(OBS)_2$ crystals at 40× precipitated from a 0.075 M SOBS/0.010 M $CaCl_2$ solution; taken after 1 wk at 30°C. For abbreviations see Figure 1.

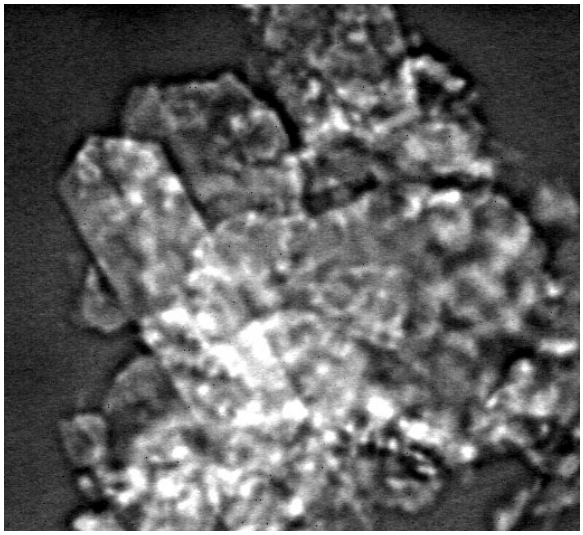

FIG. 17. Image analysis picture of crystals at 40× precipitated from a 0.012 M surfactant solution containing 83:17 SDS/SOBS and 0.008 M $CaCl_2$; taken after 1 wk at 30°C. For abbreviations see Figure 1.

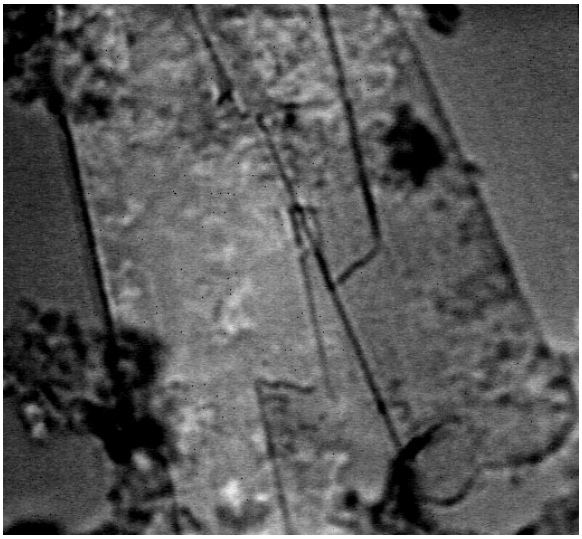

FIG. 18. Image analysis picture of crystals at 40× precipitated from a 0.014 M surfactant solution containing 71:29 SDS/SOBS and 0.008 M $CaCl_2$; taken after 1 wk at 30°C. For abbreviations see Figure 1.

sulfonate head group, whereas SDS has a 12-carbon chain and a sulfate head group. Also, the two surfactants tend to separate with time, as will be shown by image analysis pictures (as will be shown shortly). Therefore, a solid solution probably does not form between these surfactants. It has already been shown that SDS does not remain in $Ca(OBS)_2$ crystals after equilibrium has been achieved, whereas SOBS adsorbs onto the $Ca(DS)_2$ crystal surfaces. Therefore, the presence of SOBS in the $Ca(DS)_2$ crystalline phase is probably due, at least in part, to adsorption. Entrapment of mother liquor during crystallization is another likely explanation of nonequilibrium incorporation of the dissimilar surfactant in the precipitate. This latter explanation is supported by atomic force microscope pictures of the crystals (20).

Image analysis. Image analysis at 40× magnification was used to determine crystal habit for various crystals 4 min after mixing of the reactants. These pictures are shown in Figures 11–14 for 0.075 M SOBS with 0.01 M $CaCl_2$, 0.01 M SDS with 0.008 M $CaCl_2$, and the mixtures 0.01 M SDS/0.002 M SOBS (83:17 SDS/SOBS) and 0.01 M SDS/0.004 M SOBS (71:29 SDS/SOBS), each with 0.008 M $CaCl_2$. Many $Ca(OBS)_2$ crystals are elongated flat plates with jagged edges. Some jagged-edged trapezoidal shapes are present in the samples as well. The $Ca(DS)_2$ crystals are mostly trapezoidal and rhombic in shape with a few hexagonal shapes. The crystals from the mixtures are much smaller, with the crystals from the 83:17 SDS/SOBS solution mostly irregularly shaped flat plates and the crystals from the 71:29 SDS/SOBS solution more needle-like. The crystals from the mixed solutions have different crystal habits from the pure crystals. A change in crystal habit in the presence of adsorbing components is a well-documented phenomenon in the crystallization literature. Adsorption of a surfactant onto certain faces of the crystal will stunt the outward growth of that face, causing other faces to grow outward more quickly.

Image analysis was also used to view the crystals after aging for one week as shown in Figures 15–18 for 40× magnification. The crystals from 0.075 M SOBS solution and 0.01 M $CaCl_2$ are long, clear, and needle-like, as shown in Figure 15. The crystals from 0.01 M SDS solution and 0.008 M $CaCl_2$ are mostly clusters, as shown in Figure 16. The 83:17 and 71:29 SDS/SOBS mixtures seem to have both types of crystals present. There are long flat crystals similar to those seen in the pure SOBS system along with clusters as seen in the pure SDS system. The crystals from the more concentrated SDS solution seem to have more clusters present than the crystals from the less concentrated solution. The long crystals, however, do not have as well-defined shapes as in the pure $Ca(OBS)_2$ crystals. Upon ripening, at least part of the surfactant components in the crystals appear to separate into more nearly pure crystals.

ACKNOWLEDGMENTS

Financial support for this work was provided by the industrial sponsors of the Institute for Applied Surfactant Research including Akzo Nobel Chemicals Inc., Albemarle Corporation, Amway Corporation, Clorox Company, Colgate-Palmolive, Dial Corporation, Dow Chemical Company, DowElanco, E.I. DuPont de Nemours & Company, Halliburton Services Corporation, Henkel Corporation, Huntsman Corporation, ICI Americas Inc., Kerr-McGee Corporation, Lever Brothers, Lubrizol Corporation, Nikko Chemicals, Phillips Petroleum Company, Pilot Chemical Company, Proctor & Gamble Company, Reckitt Benckiser North America, Schlumberger Technology Corporation, Shell Chemical Company, Sun Chemical Corporation, Unilever Inc., and Witco Corporation.

REFERENCES

1. Rodriguez, C.H., L.H. Lowery, J.F. Scamehorn, and J.H. Harwell, Kinetics of Precipitation of Surfactants I. Anionic Surfactants with Calcium and With Cationic Surfactants, *J. Surfact. Deterg. 4*:1 (2001).
2. Clarke, D.E., R.S. Lee, and I.D. Robb, Precipitation of Calcium Salts of Surfactants, *Faraday Disc. Chem. Soc. 61*:165 (1976).
3. Lee, R.S., and I.D. Robb, Precipitation of Calcium Surfactants. Part 2, *J. Chem. Soc. Faraday Trans. 1, 75*:2116 (1979).
4. Peacock, J.M., and E. Matijevic, Precipitation of Alkylbenzene Sulfonates with Metal Ions, *J. Colloid Interface Sci. 77*:548 (1980).
5. Fan, X.J., P. Stenius, N. Kallay, and E. Matijevic, Precipitation of Surfactant Salts: II. The Effect of Nonionic Surfactants on Precipitation of Calcium Dodecyl Sulfate, *Ibid. 121*:571 (1988).
6. Stellner, K.L., and J.F. Scamehorn, Hardness Tolerance of Anionic Surfactant Solutions: 1. Anionic Surfactant with Added Monovalent Electrolyte, *Langmuir 5*:70 (1989).
7. Stellner, K.L., and J.F. Scamehorn, Hardness Tolerance of Anionic Surfactant Solutions: 2. Effect of Added Nonionic Surfactant, *Ibid. 5*:77 (1989).
8. Stellner, K.L., J.C. Amante, J.F. Scamehorn, and J.H. Harwell, Precipitation Phenomena in Mixtures of Anionic and Cationic surfactants in Aqueous Solutions, *J. Colloid Interface Sci. 123*:186 (1988).
9. Matheson, K.L., M.F. Cox, and D.L. Smith, Interactions Between Linear Alkylbenzene Sulfonates and Water Hardness Ions: I. Effect of Calcium Ion on Surfactant Solubility and Implications for Detergency Performance, *J. Am. Oil Chem. Soc., 62*:1391 (1985).

10. Matheson, K.L., Detergency Performance Comparison Between LAS and ABS Using Calcium Sulfonate Precipitation Boundary Diagrams, *Ibid. 62*:1269 (1985).
11. Scamehorn, J.F., R.S. Schechter, and W.H. Wade, Adsorption of Surfactants on Mineral Oxide Surfaces from Aqueous Solutions. I. Isomerically Pure Anionic Surfactants, *J. Colloid Interface Sci. 85*:463 (1982).
12. Scamehorn, J.F., Precipitation of Mixtures of Anionic Surfactants, in *Mixed Surfactant Systems*, edited by P.M. Holland and D.N. Rubingh, ACS Symposium Series, Vol. 501, American Chemical Society, Washington, DC, 1992, pp. 392.
13. Davies, C.W., *Ion Association*, Butterworths, London, 1962, p. 41.
14. Klotz, I.R., and R.M. Rosenberg, *Chemical Thermodynamics: Basic Theory and Methods*, 4th edn., Krieger, Malabar, 1991, pp. 440.
15. Robinson, R.A., and R.H. Stokes, *Electrolyte Solutions*, 2nd edn., Butterworths, London, 1959, pp. 174.
16. Scamehorn, J.F., and J.H. Harwell, Precipitation of Surfactant Mixtures, in *Mixed Surfactant Systems*, edited by K. Ogino and M. Abe, Marcel Dekker, New York, 1993, pp. 283.
17. Tsujii, K., N. Saito, and T. Takeuchi, Krafft Points of Anionic Surfactants and Their Mixtures with Special Attention to Their Applicability in Hard Water, *J. Phys. Chem. 84*:2287 (1980).
18. Scamehorn, J.F., An Overview of Phenomena Involving Surfactant Mixtures, in *Phenomena in Mixed Surfactant Systems*, edited by J.F. Scamehorn, ACS Symposium Series, Vol. 311, American Chemical Society, Washington, DC, 1986, pp. 1.
19. Shinoda, K., The Formation of Micelles, in *Colloidal Surfactants*, edited by K. Shinoda, T. Tamamushi, T. Nakagawa, and T. Isemura, Academic Press, New York, 1963, pp. 35.
20. Rodriguez, C.H., The Thermodynamics and Kinetics of Anionic Surfactants and Surfactant Mixtures, Ph.D. Dissertation, The University of Oklahoma, Norman, 1997.
21. Lieser, K.H., Steps in Precipitation Reactions, *Angew. Chem. Internat. Edit. 8*:188 (1969).
22. Konak, A.R., Derivation and Use of a Generalized Rate Equation for Crystallization and Precipitation, *Kristall. Technik. 9*:243 (1974).
23. Johnson, R.A., and J.D. O'Rourke, The Kinetics of Precipitate Formation: Barium Sulfate, *J. Am. Chem. Soc. 76*:2124 (1954).
24. Randolph, A.D., and M.A. Larson, *Theory of Particulate Processes*, 2nd edn., Academic Press, San Diego, 1988, pp. 109.
25. Walton, A.G., *The Formation and Properties of Precipitates*, Wiley, New York, 1967, pp. 44.
26. Mullin, J.W., *Crystallization*, 3rd edn., Butterworth-Heinemann, Boston, 1993, pp. 202.
27. Adamson, A.W., *Physical Chemistry of Surfaces*, 5th edn., Wiley, New York, 1990, pp. 291.
28. Adamson, A.W., *Physical Chemistry of Surfaces*, 5th edn., Wiley, New York, 1990, pp. 364.
29. Walton, A.G., *The Formation and Properties of Precipitates*, Wiley, New York, 1967, pp. 1.
30. Walton, A.G., *The Formation and Properties of Precipitates*, Wiley, New York, 1967, pp. 79.

[Received August 12, 1999; accepted December 5, 2000]

Cheryl Rodriguez is a scientist in the Corporate Technology Department of the Clorox Services Company. She received her B.S. and Ph.D. in chemical engineering at the University of Oklahoma. Her awards include the 1995 Ralph H. Potts Memorial Fellowship from AOCS and an Outstanding Paper Presentation at the 1996 AOCS Annual Meeting.

John Scamehorn holds the Asahi Glass Chair in Chemical Engineering and is Director of the Institute for Applied Surfactant Research at the University of Oklahoma. He received his B.S. and M.S. at the University of Nebraska and his PhD at the University of Texas, all in chemical engineering. Dr. Scamehorn has worked for Shell, Conoco, and DuPont and has been on a number of editorial boards for journals in the area of surfactants and of separation science. He has coedited four books and coauthored over 140 technical papers. His research interests include surfactant properties important in consumer product formulation and surfactant-based separation processes.